

Inhibitory effects of silibinin on proliferation and lung metastasis of human high metastasis cell line of salivary gland adenoid cystic carcinoma via autophagy induction

Canhua Jiang¹
Shufang Jin¹
Zhisheng Jiang¹
Jie Wang²

¹Department of Oral and Maxillofacial Surgery, Xiangya Hospital,

²Department of Immunology, Xiangya School of Medicine, Central South University, Changsha, Hunan, People's Republic of China

Objective: To investigate the possible mechanisms and effects of silibinin (SIL) on the proliferation and lung metastasis of human lung high metastasis cell line of salivary gland adenoid cystic carcinoma (ACC-M).

Methods: A methyl thiazolyl tetrazolium assay was performed to detect the inhibitory effects of SIL on the proliferation of ACC-M cells in vitro. Fluorescence microscopy and transmission electron microscopy were used to observe the autophagic process. Western blot was performed to detect the expression of microtubule-related protein 1 light-chain 3 (LC3). An experimental adenoid cystic carcinoma (ACC) lung metastasis model was established in nude mice to detect the impacts of SIL on lung weight and lung cancer nodules. Immunohistochemistry was used to detect the expressions of LC3 in human ACC samples and normal salivary gland tissue samples.

Results: SIL inhibited the proliferation of ACC-M cells in a dose- and time-dependent manner, and inductively increased the autophagic bodies in ACC-M cells. Furthermore, SIL could increase the expression of LC3 in ACC-M cells and promote the conversion of LC3-I into LC3-II in a dose- and time-dependent manner. In the ACC lung metastasis model, the lung weight and left and right lung nodules in the SIL-treated group were significantly less than those in the control group ($P < 0.05$). The expressions of LC3-I and LC3-II as well as the positive expression rate of LC3 (80%) significantly increased, but the positive expression of LC3 in human ACC (42.22%) reduced significantly.

Conclusion: SIL could inhibit the proliferation and lung metastasis of ACC-M cells by possibly inducing tumor cells autophagy.

Keywords: silibinin, adenoid cystic carcinoma, ACC-M cells, autophagy, microtubule-related protein 1 light-chain 3

Introduction

Silibinin (SIL) is a flavonolignan compound extracted from the fruits and seeds of *Silybum marianum*. Recent studies have found that SIL has strong antitumor activities toward a variety of epithelium-derived tumors such as colon,¹ prostate,² or lung cancer,^{3,4} and induction of tumor cell autophagy might be one of the mechanisms. Autophagy is a stress reaction of cells under starvation, hypoxia, and other internal or external environmental pressure conditions. Partial cytoplasmic matrices could be transported into lysosomes via autophagy, and their degradation products could provide substrates for anabolic metabolism and adenosine triphosphate synthesis. Autophagy is conducive for recycling cellular components, thereby maintaining homeostasis and

Correspondence: Jie Wang
Department of Immunology, Xiangya School of Medicine, Central South University, No 172 Tongzi Road, Yuelu District, Changsha 410078, Hunan, People's Republic of China
Tel/fax +86 731 8235 5010
Email jjewangdoc@163.com

survival of cells, while its dysfunction plays a major role in multiple human diseases such as cancers, neurodegenerative diseases, aging, or microbial infections.^{5,6} Adenoid cystic carcinoma (ACC) is the most common malignant tumor of the epithelial salivary glands and could easily show distant metastasis and local recurrence. Its clinical prognosis is poor and it is often fatal.⁷ ACC has been receiving increasing attention because of its unique neurotropic and high potential for lung metastasis. Most ACCs grow slowly; thus, there is a long window period for clinical intervention and measures to prevent malignancy. Therefore, exploration of new drugs that can inhibit the proliferation and lung metastasis of ACC, as well as the mechanisms underlying these processes has great significance in further improving the treatment of ACC and prolonging the survival of patients with ACC. This study investigated the impacts of SIL on the proliferation and lung metastasis of human lung high metastasis cell line of salivary gland adenoid cystic carcinoma (ACC-M) cells and the possible underlying mechanisms. The results revealed that SIL could inhibit the *in vitro* proliferation of ACC-M cells and induce autophagy. SIL could also inhibit lung metastasis of ACC-M cells in an experimental nude mouse model and induce autophagy in pulmonary metastatic tissues. Furthermore, our study also found that the positive expression rate of light-chain 3 (LC3), an autophagy-related protein, in ACC patients was lower than that in the normal glandular tissues, suggesting that SIL could inhibit the proliferation and lung metastasis of ACC-M cells via autophagy induction. Therefore, because of its low toxicity and antitumor effects, SIL has the potential to become a new therapeutic option for ACC.

Materials and methods

Methyl thiazolyl tetrazolium (MTT) assay

The ACC-M cells (catalog number GDC066) were provided by the China Center for Type Culture Collection, Wuhan University (Wuhan, People's Republic of China). They were screened through five consecutive passages in nude mice *in vivo* at the College of Stomatology, Shanghai Jiao Tong University (Shanghai, People's Republic of China).⁸ The cells were conventionally cultured in Roswell Park Memorial Institute 1640 culture medium (Hyclone, Logan, UT, USA) containing 10% fetal bovine serum (Hyclone) at 37°C and 5% CO₂. The ACC-M cells in the logarithmic growth phase were then harvested, and the cell density was adjusted to 2.5×10⁴/mL, followed by seeding into 96-well plates (150 µL per well). Each well was setup with five parallel wells and a negative control. After culturing for 24 hours at 37°C under 5% CO₂, different concentrations of SIL were added. The final

concentrations of SIL (Sigma-Aldrich, St Louis, MO, USA) used were 20, 40, 80, 120, and 160 µg/mL, which were then cultured for 24, 48, and 72 hours, respectively. Subsequently, 15 µL of MTT (Sigma-Aldrich) (5 mg/mL) was added to each well and recultured/incubated for another 4 hours, after which the supernatant was sucked and discarded; 150 µL of dimethyl sulfoxide (Sigma-Aldrich) was then added into each well. After slightly shaking the cultures for 10 minutes on a shaking table to completely dissolve the crystals, the absorbance of each well (optical density) at 570 nm was measured with one microplate reader (Molecular Devices, Ramsey, MN, USA); the cell growth curve was then drawn based on the absorbance values.

Observation of cell autophagy by monodansyl cadaverine (MDC) staining

According to a previous report,⁹ the ACC-M cells in the logarithmic growth phase were harvested, and the cell concentration was adjusted to 1×10⁵/mL and seeded in cover slip containing 12-well plates for a 24-hour culture; SIL was then added at a final concentration of 80 µg/mL for a 24-hour culture. After discarding the supernatant, 0.05 mM MDC (Sigma-Aldrich) was added to the cells and cultured at 37°C in darkness for 10 minutes. After washing the ACC-M cells four times with 4°C phosphate-buffered saline for 5 minutes, the cover slips paved with the ACC-M cells were directly covered upside down on the slide for an instant observation and photography using a fluorescence microscope (Olympus, Melville, NY, USA) with excitation and emission wavelengths of 380 and 525 nm, respectively.

Transmission electron microscope (TEM)

The ACC-M cells in the logarithmic growth phase were harvested and cultured with SIL (80 µg/mL) for 24 hours. The cells were then subjected to the following processes: fixation, gradient dehydration, soaking with 1:1 epoxy resin mixture and pure acetone, embedding, sectioning, and lead acetate–lead nitrate dual staining. The cells were afterward observed and photographed under a TEM (Olympus).

Animal grouping and processing

Twenty BALB/c nu/nu mice (15–25 g, 3–4 weeks old, male: female =1:1) were provided by the Experimental Animal Center of Central South University. After being fed for a week under specific pathogen-free conditions, these mice were randomly divided into two groups (n=10, male:female=1:1). Each mouse was injected with 0.2 mL of ACC-M cell suspension (1×10⁶/mL) via the tail vein. After 24 hours, the mice in the experimental group were intraperitoneally

injected with 0.8 mL of 1 mg/mL SIL solution daily while the control group was injected with the same volume of an Roswell Park Memorial Institute 1640 medium. After 6 weeks, all mice were sacrificed by cervical dislocation and the lungs were then removed, cleaned, and weighed to calculate the number of bi-lung tumor nodules. The left lung tumor nodules were then separated and stored in liquid nitrogen for Western blot analysis; the remaining lung tissues were subjected to formalin fixation and paraffin embedding for the subsequent immunohistochemical assay. This study was carried out in strict accordance with the recommendations in the Guide for the Care and Use of Laboratory Animals of the National Institutes of Health. The study was reviewed and approved by the Institutional Animal Care and Use Committee of the Central South University.

Western blot

The radioimmunoprecipitation assay (Sigma-Aldrich) lysate and phenylmethylsulfonyl fluoride (Sigma-Aldrich) were mixed to extract the total proteins from the SIL-treated ACC-M cells and the lung metastases of ACC nude mice. The bicinchoninic acid method was used to detect the total proteins. The proteins were then mixed with 2× sodium dodecyl sulfate loading buffer and heated until denaturation. Fifty micrograms of proteins was loaded into each lane for a 12% sodium dodecyl sulfate polyacrylamide gel electrophoresis. Afterward, the proteins were transferred onto one polyvinylidene difluoride membrane, followed by closure with 3% skimmed milk at room temperature overnight; the primary antibodies (anti-β-actin antibody (Abgent, San Diego, CA, USA): diluted with Tris-buffered saline and tween 20 (TBST), 1:2,000; anti-LC3 antibody (Abgent): diluted with TBST, 1:500) were then added and incubated at 4°C overnight. After washing with TBST three times (slightly pendulated for 10 minutes each time), an horse radish peroxidase-conjugated goat antimouse IgG (Abgent) (dilution with TBST, 1:2,000) was added and incubated at room temperature for 1 hour. After subsequently washing with TBST three times for 10 minutes, the ECL kit (Santa Cruz Biotechnology, Santa Cruz, CA, USA) was used for coloration and the films were then developed in darkness.

Immunohistochemistry

The paraffin-embedded ACC specimens, as well as the complete clinical data of 45 patients treated in the Department of Oral and Maxillofacial Surgery, Xiangya Hospital, Central South University, from January 2006 to 2012 were collected. All the patients were not subjected to

preoperative radiotherapy and chemotherapy. Furthermore, 23 normal salivary gland specimens were obtained, which were resected due to benign tumor, 1.0 cm away from the tumor border, and showed no inflammatory cell infiltration after hematoxylin and eosin staining. The collection of all the specimens was approved by the ethics committee of Xiangya Hospital.

The paraffin-embedded specimens of the ACC, normal salivary gland, and lung metastatic tissues in the ACC nude mice were treated in the following processes in turn: conventional slicing, dewaxing, hydration, endogenous peroxidase removal with 3% H₂O₂, microwave antigen retrieval, 2-hour calf serum closure, and overnight incubation with LC3 rabbit polyclonal antibody (NOVUS Co., Littleton, CO, USA) at 4°C. Fifty microliters of the horse radish peroxidase-conjugated goat antirabbit IgG secondary antibody (Abgent) working solution was then added dropwise and incubated at 37°C for 30 minutes, followed by diaminobenzidine (Sigma-Aldrich) coloration, hematoxylin restaining, hydrochloric acid differentiation, saturated lithium carbonate re-blue-staining, gradient alcohol dehydration, xylene hyalinization, and neutral resin mounting in turns. Phosphate-buffered saline was used to replace the primary antibody for the negative control.

Determination of immunohistochemical staining results: all the slices were reviewed by two pathologists independently according to the blind method, and the appearance of brown particles in the cytoplasm was determined as positive. Five high-power fields were randomly selected for the observation, and 100 cells were selected from each field for the counting. The following results were finally comprehensively evaluated according to the positive cell rate and the staining intensity: 1) scores of the positive cell ratio (to the overall cells): 0 point: <10%, 1 point: 10%–25%, 2 points: 26%–50%, 3 points: >50%; 2) scores of the staining intensity: 0 point: nonstained, 1 point: pale yellow, 3 points: yellow to brown, 2 points: between 1 and 3 points; 3) total score = the score of the positive cell ratio × the score of staining intensity: 0–1 point: negative, 2–3 points: weak positive, 4–5 points: moderate-strong positive, >6 points: strong positive.

Statistical analysis

SPSS 13.0 (SPSS Inc., Chicago, IL, USA) statistical software was used for the statistical analysis. For multigroup comparison, analysis of variance was used, whereas for comparison of intergroup measurement data, the *t*-test with heterogeneity of variance was used; the counting data were performed using the Fisher's exact test, followed by the χ^2 test, with $P < 0.05$ considered as statistically significant.

Results

SIL inhibited the proliferation of the ACC-M cells

MTT assay showed that under low dose (20 and 40 $\mu\text{g/mL}$) and short intervention time (24 hours) conditions, SIL showed no obvious influence on the proliferation of the ACC-M cells. When the dose was increased (≥ 80 $\mu\text{g/mL}$), SIL significantly inhibited the proliferation of the ACC-M cells ($P < 0.05$), and this inhibitory effect became more significant with an increase in time (48 and 72 hours) (Figure 1).

SIL could induce the autophagy of ACC-M cells

MDC is a marker of autophagy, which can selectively bind with the intracellular autophagic vacuoles (AVs), thus exhibiting spotty bright green fluorescence around the nuclei and in the cytoplasm under an excitation wavelength. The exposure of ACC-M cells to 80 $\mu\text{g/mL}$ SIL for 24 hours significantly increased the green fluorescent spots around the nuclei and in the cytoplasm (Figure 2A), indicating that SIL could induce the ACC-M cells to produce AVs. Examination by TEM showed that, in the control group, the cells had large nuclei, a clear nuclear membrane, a high nuclear/cytoplasm ratio, aside shifted nucleoli, even cytoplasmic matrix density, and microvilli on the cell surface. After the exposure of ACC-M cells to 80 $\mu\text{g/mL}$ SIL for 24 hours, the nuclear/cytoplasm ratio decreased and vacuoles of various sizes were observed

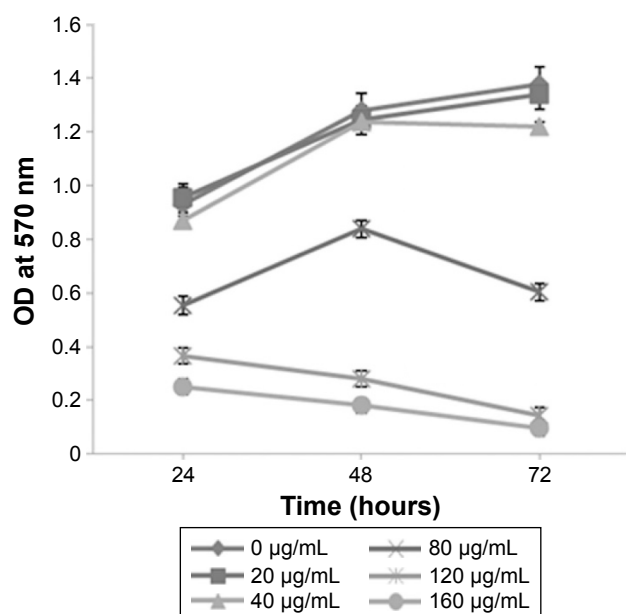


Figure 1 Impacts of SIL on the proliferation of the ACC-M cells by MTT assay. **Abbreviations:** ACC-M, human lung high metastasis cell line of salivary gland adenoid cystic carcinoma; MTT, methyl thiazolyl tetrazolium; OD, optical density; SIL, silibinin.

in the cytoplasm. In addition, the cytoplasm partially dissolved, AVs appeared, and even necrotic organelles could be seen in partial AVs. Furthermore, the microvilli of the cell surface became shorter (Figure 2B). Western blot assay revealed that after different concentrations of SIL (40, 80, 120, and 160 $\mu\text{g/mL}$) acted on the ACC-M cell for 24 hours, the expressions of LC3-I and LC3-II increased with an increase in the concentration while the LC3-II/LC3-I ratio also increased. After 100 $\mu\text{g/mL}$ SIL acted on the ACC-M cells for 48 hours, the expressions of LC3-I and LC3-II were stronger than those subjected to a 24-hour intervention, and so was the ratio of LC3-II/LC3-I. The results suggested that SIL could increase the expression of autophagy-related LC3 proteins in a dose- and time-dependent manner as well as promote the conversion of LC3-I to LC3-II (Figure 2C).

SIL inhibited the experimental lung metastasis

After 1×10^6 ACC-M cells were injected via the tail vein for 6 weeks, the success rate of the lung metastasis in the nude mice was found to be 100%; all the mice exhibited tumor nodules in both right and left lung, indicating that the experimental lung metastasis of ACC in nude mice was successfully established. The lung weights in the control group and the SIL-treated group were (4.20 ± 0.06) and (4.08 ± 0.11) g, respectively. The left and right lung tumor nodules in the control group were (9.29 ± 5.91) and (10.71 ± 7.83) , respectively, whereas those in the SIL-treatment group were (3.11 ± 3.76) and (2.22 ± 3.46) , respectively. The lung weight and the left and right lung tumor nodules in the SIL-treated group were significantly lower than the control group ($P < 0.05$) statistically (Table 1; Figure 3). The results suggested that SIL could inhibit the experimental lung metastasis of ACC in nude mice.

SIL upregulated the expression of autophagy-related protein LC3

Western blot revealed that the relative expressions of LC3-I and LC3-II proteins in the SIL-treated group were higher than in the control group (Figure 4A, $P < 0.05$). The immunohistochemical assay revealed that LC3 was commonly expressed in the cytoplasm, thus staining the cytoplasm yellow or brown. The positive expression rate of LC3 in the SIL-treated group was 80% (8/10), which was statistically higher than that of the control group (30%, 3/10, $P < 0.05$) (Figure 4B; Table 2).

The positive expression rate of LC3

The immunohistochemical assay revealed that the positive LC3 rate in the 45 ACC specimens (42.22%) was significantly

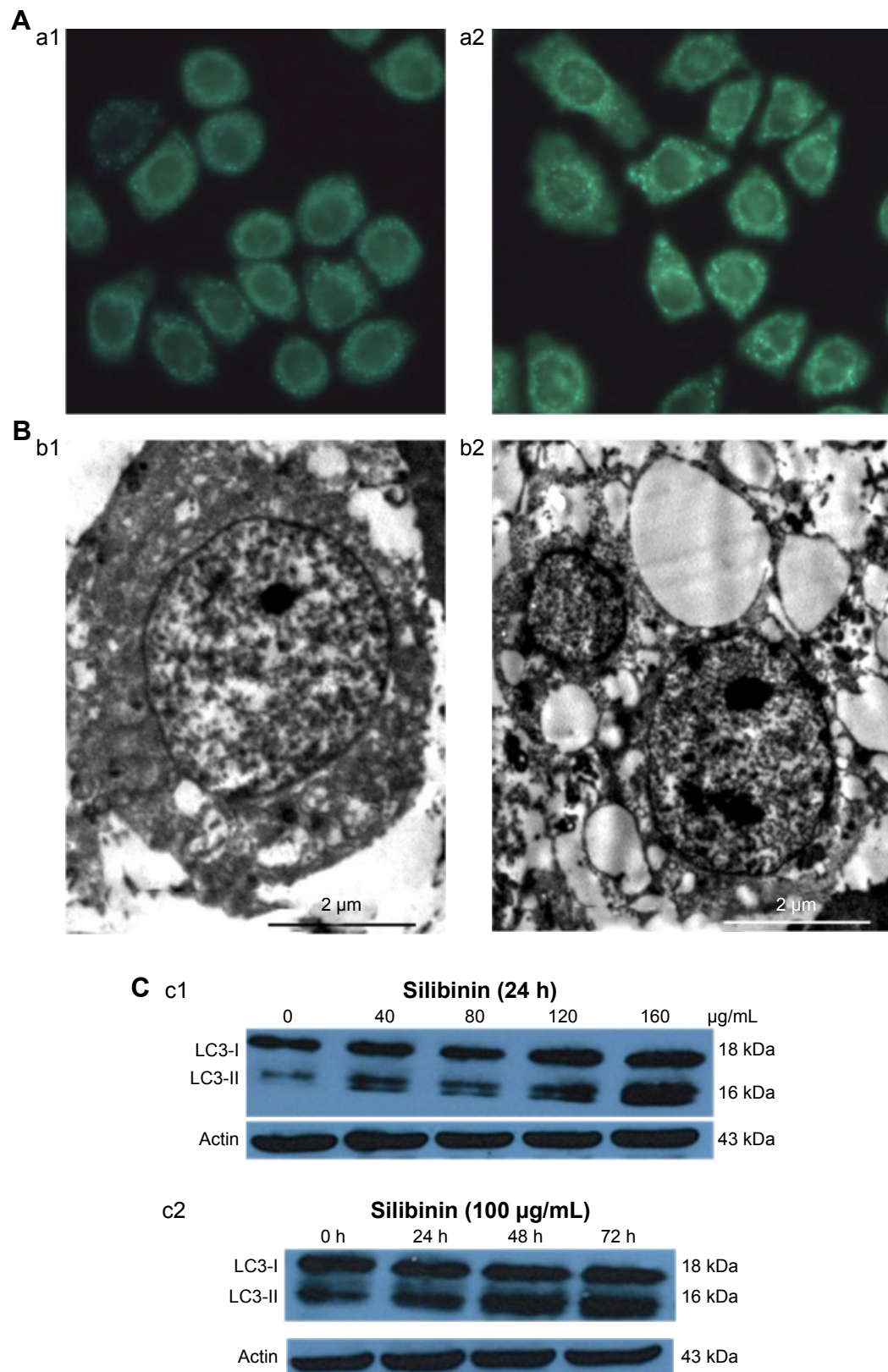


Figure 2 SIL induced the autophagy of the ACC-M cells.

Notes: (A) AVs detection by MDC staining (fluorescence microscope, $\times 200$). (a1) The control group; (a2) the SIL-treatment groups, 80 $\mu\text{g/mL}$. (B) Ultrastructures of AVs by TEM. (b1) The control group: clear nucleoli, large nuclear/cytoplasm ratio, aside-shifted nucleoli, even cytoplasm matrix density ($\times 5,000$); (b2) AVs in the cells of the SIL-treatment group ($\times 5,000$). (C) Expression detection of LC3-I and LC3-II by Western blot. (c1) Expressions after cultured with different concentrations of SIL for 24 hours; (c2) expressions of LC3-I and LC3-II after 100 $\mu\text{g/mL}$ of SIL acted on the ACC-M cells at different time periods.

Abbreviations: ACC-M, human lung high metastasis cell line of salivary gland adenoid cystic carcinoma; AVs, autophagic vacuoles; LC3, light-chain 3; MDC, monodansyl cadaverine; SIL, silibinin; TEM, transmission electron microscopy.

Table 1 Comparison of lung weight and lung tumor nodules between the two groups

Group	Lung weight (g)	Left lung tumor nodules (pieces)	Right lung tumor nodules (pieces)
SIL	4.08±0.11*	3.11±3.76*	2.22±3.46*
Control	4.20±0.06	9.29±5.91	10.71±7.83
P-value	0.035	0.023	0.029

Notes: Data presented as mean ± standard deviation. *Significant difference when compared with the control group, $P < 0.05$.

Abbreviation: SIL, silibinin.

lower than that in the 23 normal salivary gland specimens (91.30%) (Table 3, $P < 0.05$).

Among the 45 ACC specimens, 19 (42.22%) specimens exhibited positive LC3 expression in the cytoplasm and partial nuclei; the expression level was lower, mainly weak positive (16/45, 35.36%), and the positive result accounted for 6.67% (3/45); 26 specimens showed no LC3 protein expression (57.78%). Among the 23 normal salivary gland specimens, 21 (91.30%) specimens exhibited positive LC3 expression in the cytoplasm and nuclei; the expression level were higher, and mainly strong positive (10/23, 43.49%), positive (6/23, 26.09%), and weak positive results only accounted for 21.74% (5/23); two specimens showed no LC3 protein expression (8.70%) (Figures 5 and 6).

Discussion

ACC originates from the intercalated duct reserve cells, and typically develops in the salivary gland tissue. Currently, the treatment of ACC involves surgical resection and is assisted by radiotherapy. However, due to the biological characteristics of neutrophils and the special structures of head and neck, clinicians have great difficulty in determining the precise extent of tumor resection feasible. If the resection is inadequate, postoperative recurrence might occur; however, blindly expanding the resection range would inevitably

sacrifice the adjacent important organs and tissues, thus causing severe deformity and dysfunction. The response rates of ACC to single radiotherapy and conventional chemotherapy are relatively low; thus, exploring a low toxicity antitumor drug is very necessary.

In vitro and in vivo experiments have revealed that some natural compounds could exert antitumor effects such as inhibiting cell proliferation, inducing apoptosis, inhibiting angiogenesis, delaying metastasis, and improving sensitivity of certain chemical drugs; hence, extracting low toxicity natural drug compounds from plants that could inhibit mitosis of tumor cells and cell growth signaling pathways has become a hot research topic recently, and SIL is one of them.¹⁰⁻¹² Recent studies have found that SIL has strong antitumor activities toward a variety of epithelium-derived tumors, such as prostate,² colon,¹ bladder,¹³ breast,¹⁴ ovarian,¹⁵ and lung cancers.^{3,4} This study analyzed the impacts of SIL on the proliferation of ACC-M cells, and the results revealed that SIL could inhibit the proliferation of ACC-M cells in time- and dose-dependent manner, particularly when treated with 160 µg/mL of SIL for 72 hours, the inhibition rate of 93% suggested that SIL had significant inhibitory activities toward ACC. Lung metastasis is another clinicopathological feature of ACC, which might appear in the early stage or even several years after the primary tumor is resected. This study found that after injecting the ACC-M cells via the tail vein for 6 weeks, the lung metastasis rate of ACC in nude mice was 100%, with all the mice exhibiting the formation of lung tumor nodules that indicated that the experimental lung metastasis model of ACC in nude mice was successfully established. The lung weight and the left and right lung tumor nodules in the SIL-treated group were significantly lower than that of the control group ($P < 0.05$), indicating that SIL could inhibit the experimental lung metastasis of ACC-M cells in

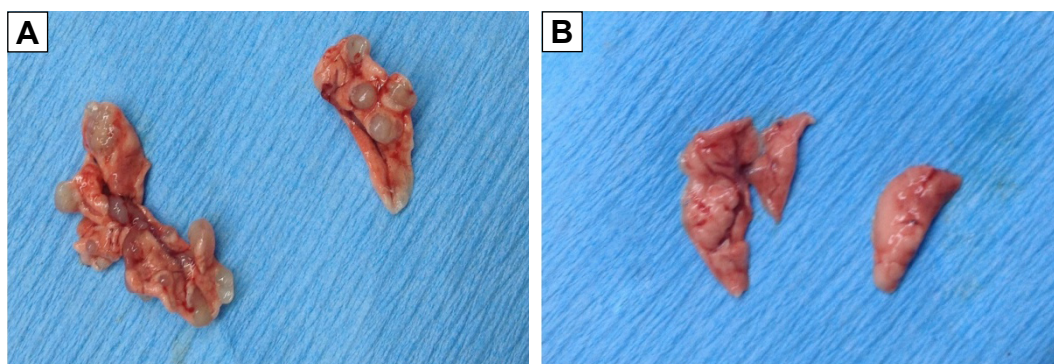


Figure 3 Lung metastatic nodules in the SIL-treatment group.

Notes: (A) Lung metastatic nodules in the control group. (B) Lung metastatic nodules in the SIL-treatment group.

Abbreviation: SIL, silibinin.

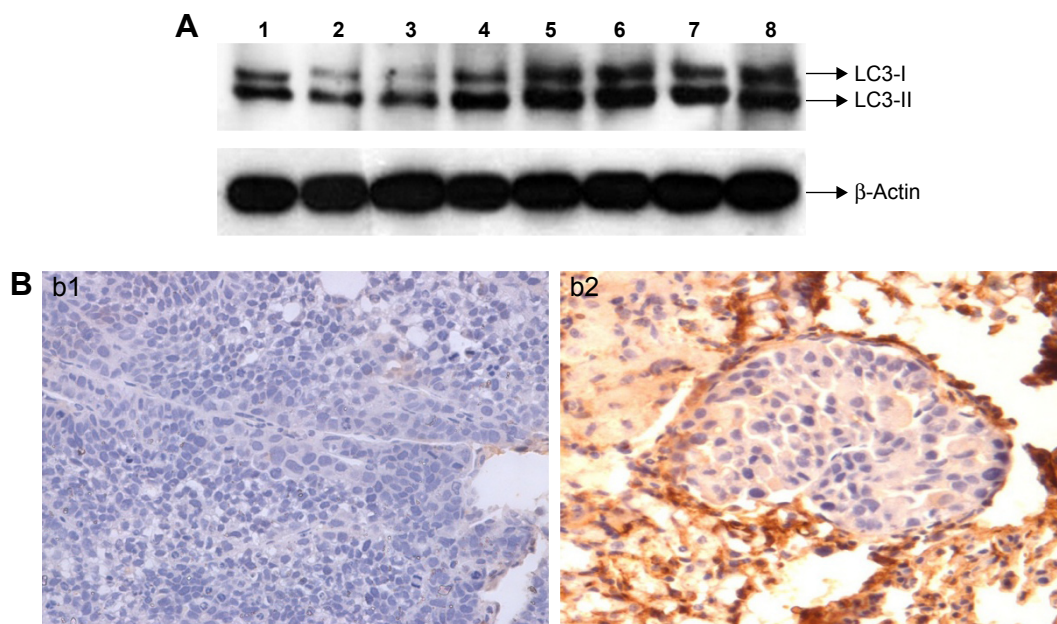


Figure 4 SIL upregulated the expression of autophagy-related protein LC3 in the experimental lung metastasis of ACC in nude mice.

Notes: (A) Western blot. 1–4: control group, 5–8: SIL-treatment group. (B) Immunohistochemical staining ($\times 200$). (b1) LC3 was negatively expressed in the control group; (b2) LC3 was positively expressed in the SIL-treatment group.

Abbreviations: ACC, adenoid cystic carcinoma; LC3, light-chain 3; SIL, silibinin.

ACC nude mice, and SIL could be expected to become a new antitumor treatment for ACC. The mechanism of SIL in inhibiting tumor growth has not been fully elucidated, and there is no consensus on the mechanism of action of SIL in different tumors. Previous literature^{16–19} have reported that SIL can reduce the activities of matrix metalloproteinase-2, matrix metalloproteinase-9, and urokinase plasminogen activator in tumor cells, and inhibit the expression of cell cycle protein, thus inhibiting tumor growth. The inhibitory effects of SIL on proliferation and lung metastasis of ACC-M need to be further explored.

Current studies have shown that many anticancer measures could induce autophagy, indicating that autophagic cell death is an important mechanism of these measures. The anticancer measures that could induce autophagy include the following: radiation, rapamycin, histone deacetylase inhibitors, arsenic trioxide, temozolomide, or vitamin D analogs.²⁰ Recently, Kim et al²¹ reported that SIL could

induce the autophagy of prostate cancer (PC-3) cells, and the autophagy-specific inhibitor 3-methyl adenine could block SIL-induced PC-3 autophagy. The application of active oxygen inhibitor diphenyleneiodonium further confirmed that SIL could induce autophagy by inducing nitric oxide synthase. The results of this study also showed that after SIL induction, AVs in the ACC-M cells increased, the expressions of LC3-I and LC3-II proteins in the ACC-M cells were upregulated, and the ratio of LC3-II/LC3-I increased with increasing SIL-intervention-dosage and time. In the experimental lung metastasis model in ACC nude mice, the relative expression levels of LC3-I and LC3-II proteins in the lung metastases of the SIL-treated group were significantly higher ($P < 0.05$), and the immunohistochemical assay also showed that positive LC3 expression rate in the lung metastases of the SIL-treatment group (80%) was significantly higher than the control group (30%) ($P < 0.05$).

Table 2 Comparison of positive LC3 expression rates in the lung metastatic tissues between the two groups

Group	Cases	LC3		χ^2	P-value
		Positive	Negative		
SIL treatment	10	8	2	10	0.002
Control	10	3	7		

Abbreviations: LC3, light-chain 3; SIL, silibinin.

Table 3 Expressions of LC3 in ACC specimens and normal salivary gland specimens

Group	Cases	Expression intensity of LC3				Positive rate (%)
		-	+	++	+++	
ACC	45	26	16	3	0	42.22*
Normal salivary gland specimen	23	2	5	6	10	91.30

Note: *Significant difference when compared with the control group, $P < 0.05$.

Abbreviations: ACC, adenoid cystic carcinoma; LC3, light-chain 3.

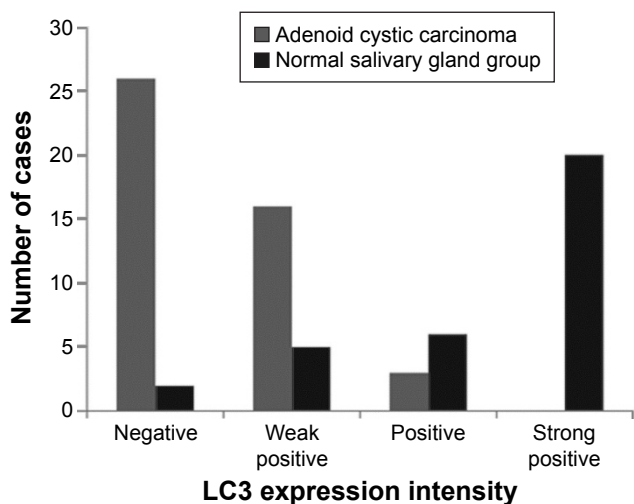


Figure 5 LC3 expressions in the ACC tissues and the normal glandular tissues. **Abbreviations:** ACC, adenoid cystic carcinoma; LC3, light-chain 3.

These results suggested that SIL could induce autophagy in ACC-M cells and lung metastatic tissues.

Autophagy could inhibit tumor development, and it might be one of the possible inhibition mechanisms of certain drugs toward tumors. Xing et al²² pointed out that a number of

anticancer drugs, such as paclitaxel and vinblastine, could make stomach cancer cells to undergo autophagy and then die. One study about papillary thyroid cancer cells²³ showed that autophagy inhibitors could promote resistance of papillary thyroid cancer cells to doxorubicin and radiotherapy. Autophagy could also inhibit the inflammatory response caused by infiltration of macrophages, thus preventing the metastasis of tumor cells and inducing the release of immunomodulatory cytokines to stimulate the body to produce antitumor immunity; meanwhile, autophagy could promote cell dormancy so as to inhibit tumor metastasis.²⁴ We used an immunohistochemical method to detect the positive expression rate of LC3 and found that the expression rate in ACC (42.22%) was significantly lower than that in normal salivary gland tissues (91.30%) ($P < 0.05$), indicating that autophagy might be related to the occurrence and development of ACC. Coupled with the results that SIL could induce autophagy of ACC, as well as inhibit the proliferation and lung metastasis of ACC-M cells in nude mice, we could conclude that SIL might inhibit the proliferation and lung metastasis of ACC cells through autophagy induction. Therefore, this study

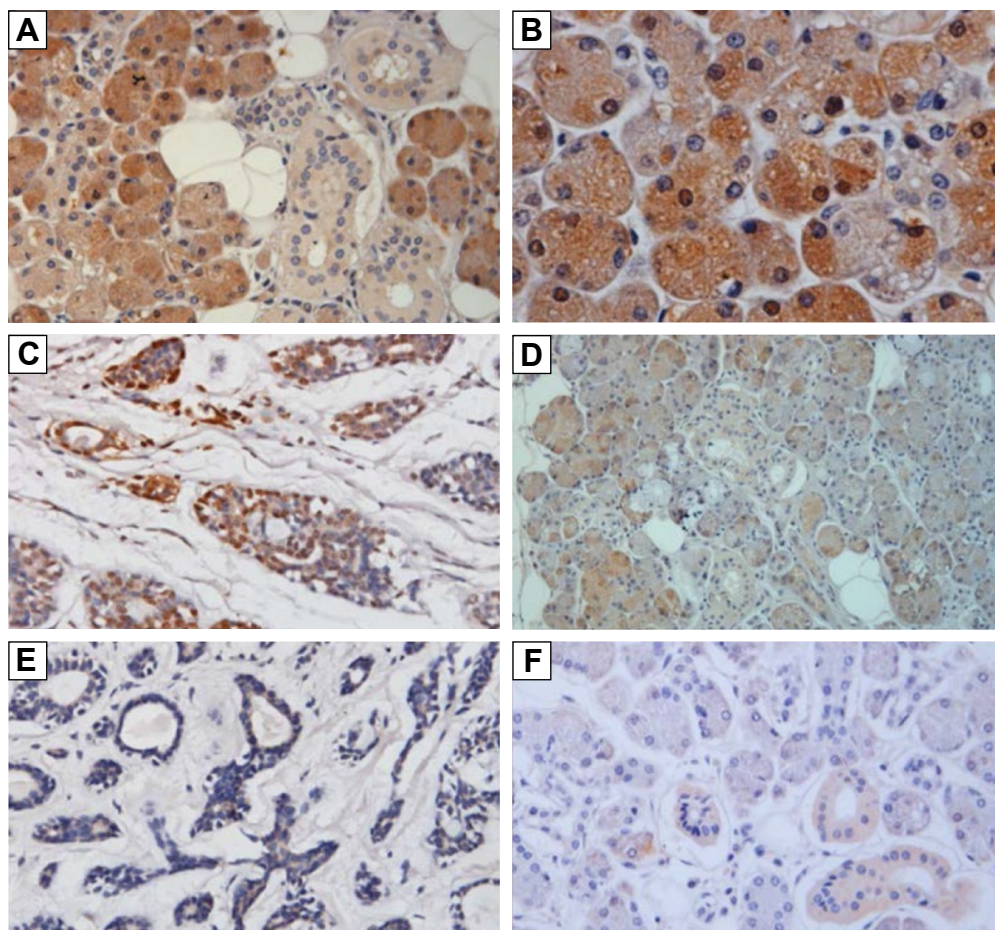


Figure 6 (Continued)

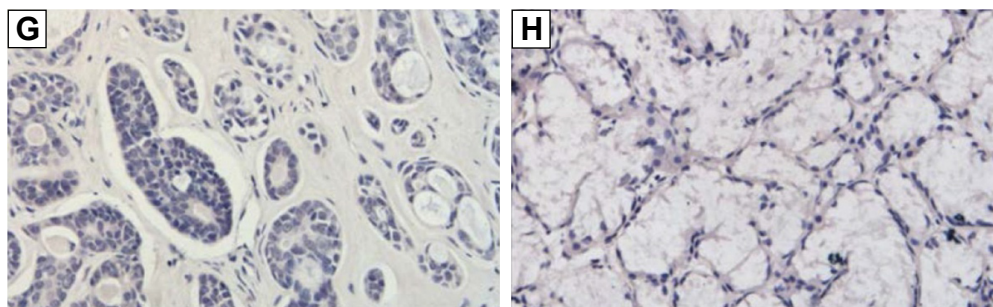


Figure 6 Expression of LC3 in salivary gland ACC and normal salivary gland tissues (IHC, SP).

Notes: (A) Strong-positive LC3 expression in normal salivary gland tissues ($\times 200$). (B) Strong-positive LC3 expression in normal salivary gland tissues ($\times 400$). (C) Middle-positive LC3 expression in ACC ($\times 200$). (D) Middle-positive LC3 expression in normal salivary gland tissues ($\times 200$). (E) Weak-positive LC3 expression in ACC ($\times 200$). (F) Weak-positive LC3 expression in normal salivary gland tissues ($\times 200$). (G) Negative LC3 expression in ACC ($\times 200$). (H) Negative LC3 expression in normal salivary gland tissues ($\times 200$).

Abbreviations: ACC, adenoid cystic carcinoma; IHC; immunohistochemistry; LC3, light-chain 3; SP, streptavidin peroxidase conjugate method.

provided new clues and an experimental basis for applying SIL for the clinical treatment of ACC.

Currently, different institutes have obtained inconsistent results about the roles of autophagy in the occurrence and development of tumors as well as its therapeutic effects due to their different research directions.^{25–27} It was found that the roles of autophagy dynamically changed with changes in tumors. During the early stages of autophagy, a tumor cell's ability to continuously proliferate reduces due to decreased protein degradation and increased synthesis, making autophagy act as an inhibitory factor toward tumorigenesis, thus inhibiting the tumors. However, when the tumor grows to a certain stage, many blood vessels might proliferate around the tumor, resulting in nutritional deficiencies, insufficient support, and necrosis in the tumor cells, during which autophagy could make the tumor cells to survive and avoid necrosis in such environments. During this period, autophagy acts as a contributing factor toward tumorigenesis. Autophagy's ability to block necrosis and inflammations limits the invasion and spread of tumor cells from the primary area; therefore, in the early stage, autophagy could inhibit a tumor's metastasis. On the other hand, autophagy might promote metastasis during the advanced stage, which manifests when confronting cells or metabolic stress. The tumor cells could spread to distant organs through the vasculature, and during this process, autophagy plays a protective role. Therefore, accurately determining the roles of autophagy in different tumors and at different stages of the same tumor has great significance toward treatment. In this study, when the mice had been injected with ACC-M cells via the tail vein for 24 hours, namely in the early tumor stage, the administration of SIL induced autophagy to play the role of inhibiting the tumor. However, further studies are necessary to determine whether SIL intervention could still

inhibit the ACC cells or play the promotive effects when the tumor developed into a certain stage.

Acknowledgment

This study was funded by the National Natural Science Foundation of China (81271154).

Disclosure

The authors report no conflicts of interest in this work.

References

1. León IE, Cadavid-Vargas JF, Tiscornia I, et al. Oxidovanadium (IV) complexes with chrysin and silibinin: anticancer activity and mechanisms of action in a human colon adenocarcinoma model. *J Biol Inorg Chem*. 2015;20(7):1175–1191.
2. Prajapati V, Kale RK, Singh RP. Silibinin combination with arsenic strongly inhibits survival and invasiveness of human prostate carcinoma cells. *Nutr Cancer*. 2015;67(4):647–658.
3. Sadava D, Kane SE. Silibinin reverses drug resistance in human small-cell lung carcinoma cells. *Cancer Lett*. 2013;339(1):102–106.
4. Mateen S, Raina K, Agarwal R. Chemopreventive and anti-cancer efficacy of silibinin against growth and progression of lung cancer. *Nutr Cancer*. 2013;65(Suppl 1):3–11.
5. Levine B, Kroemer G. Autophagy in the pathogenesis of disease. *Cell*. 2008;132(1):27–42.
6. Choi AM, Ryter SW, Levine B. Autophagy in human health and disease. *N Engl J Med*. 2013;368(7):651–662.
7. Coca-Pelaz A, Rodrigo JP, Bradley PJ, et al. Adenoid cystic carcinoma of the head and neck – An update. *Oral Oncol*. 2015;51(7):652–661.
8. Guan X, Qiu W, He R. The selection of highly lung metastatic salivary adenoid cystic carcinoma clone. *Zhong Hua Kou Qiang Yi Xue Za Zhi*. 1996;31(2):74–77. Chinese.
9. Munafó DB, Colombo MI. A novel assay to study autophagy: regulation of autophagosome vacuole size by amino acid deprivation. *J Cell Sci*. 2001;114(20):3619–3629.
10. Cheung CW, Gibbons N, Johnson DW, Nicol DL. Silibinin – a promising new treatment for cancer. *Anticancer Agents Med Chem*. 2010;10(3):186–195.
11. Gazák R, Walterová D, Kren V. Silybin and silymarin – new and emerging applications in medicine. *Curr Med Chem*. 2007;14(3):315–338.
12. Bosch-Barrera J, Menendez JA. Silibinin and STAT3: a natural way of targeting transcription factors for cancer therapy. *Cancer Treat Rev*. 2015;41(6):540–546.

13. Wu K, Ning Z, Zeng J, et al. Silibinin inhibits β -catenin/ZEB1 signaling and suppresses bladder cancer metastasis via dual-blocking epithelial-mesenchymal transition and stemness. *Cell Signal*. 2013; 25(12):2625–2633.
14. Zheng N, Zhang P, Huang H, et al. ER α down-regulation plays a key role in silibinin-induced autophagy and apoptosis in human breast cancer MCF-7 cells. *J Pharmacol Sci*. 2015;128(3):97–107.
15. Cho HJ, Suh DS, Moon SH, et al. Silibinin inhibits tumor growth through downregulation of extracellular signal-regulated kinase and Akt in vitro and in vivo in human ovarian cancer cells. *J Agric Food Chem*. 2013;61(17):4089–4096.
16. Chen PN, Hsieh YS, Chiang CL, Chiou HL, Yang SF, Chu SC. Silibinin inhibits invasion of oral cancer cells by suppressing the MAPK pathway. *J Dent Res*. 2006;85(3):220–225.
17. Chu SC, Chiou HL, Chen PN, Yang SF, Hsieh YS. Silibinin inhibits the invasion of human lung cancer cells via decreased productions of urokinase-plasminogen activator and matrix metalloproteinase-2. *Mol Carcinog*. 2004;40(3):143–149.
18. Hsieh YS, Chu SC, Yang SF, Chen PN, Liu YC, Lu KH. Silibinin suppresses human osteosarcoma MG-63 cell invasion by inhibiting the ERK-dependent c-Jun/AP-1 induction of MMP-2. *Carcinogenesis*. 2007; 28(5):977–987.
19. Kim S, Choi MG, Lee HS, et al. Silibinin suppresses TNF-alpha-induced MMP-9 expression in gastric cancer cells through inhibition of the MAPK pathway. *Molecules*. 2009;14(11):4300–4311.
20. Hippert MM, O'Toole PS, Thorburn A. Autophagy in cancer: good, bad, or both? *Cancer Res*. 2006;66(19):9349–9351.
21. Kim SH, Kim KY, Yu SN, et al. Autophagy inhibition enhances silibinin-induced apoptosis by regulating reactive oxygen species production in human prostate cancer PC-3 cells. *Biochem Biophys Res Commun*. 2015;468(1–2):151–156.
22. Xing C, Zhu B, Liu H, Yao H, Zhang L. Class I phosphatidylinositol 3-kinase inhibitor LY294002 activates autophagy and induces apoptosis through p53 pathway in gastric cancer cell line SGC7901. *Acta Biochim Biophys Sin (Shanghai)*. 2008;40(3):194–201.
23. Lin CI, Whang EE, Abramson MA, et al. Autophagy: a new target for advanced papillary thyroid cancer therapy. *Surgery*. 2009; 146(6):1208–1214.
24. Sosa MS, Bragado P, Debnath J, Aguirre-Ghiso JA. Regulation of tumor cell dormancy by tissue microenvironments and autophagy. *Adv Exp Med Biol*. 2013;734:73–89.
25. Ma B, Liang LZ, Liao GQ, et al. Inhibition of autophagy enhances cisplatin cytotoxicity in human adenoid cystic carcinoma cells of salivary glands. *J Oral Pathol Med*. 2013;42(10):774–780.
26. Liang DH, El-Zein R, Dave B. Autophagy inhibition to increase radiosensitization in breast cancer. *J Nucl Med Radiat Ther*. Epub 2015 Sep 28.
27. Kroemer G, Galluzzi L, Kepp O, Zitvogel L. Immunogenic cell death in cancer therapy. *Annu Rev Immunol*. 2013;31:51–72.

OncoTargets and Therapy

Publish your work in this journal

OncoTargets and Therapy is an international, peer-reviewed, open access journal focusing on the pathological basis of all cancers, potential targets for therapy and treatment protocols employed to improve the management of cancer patients. The journal also focuses on the impact of management programs and new therapeutic agents and protocols on

Submit your manuscript here: <http://www.dovepress.com/oncotargets-and-therapy-journal>

patient perspectives such as quality of life, adherence and satisfaction. The manuscript management system is completely online and includes a very quick and fair peer-review system, which is all easy to use. Visit <http://www.dovepress.com/testimonials.php> to read real quotes from published authors.

Dovepress